Electric Power Systems Research 235 (2024) 110709

Contents lists available at ScienceDirect

Electric Power Systems Research

journal homepage: www.elsevier.com/locate/epsr

Power grid parameter estimation without phase measurements: Theory and empirical validation☆

Jean-Sébastien Brouillon [a,*], Keith Moffat [b], Florian Dörfler [b], Giancarlo Ferrari-Trecate [a]

[a] Institute of Mechanical Engineering, Ecole Polytechnique Fédérale de Lausanne, Lausanne, Switzerland
[b] Department of Information Technology and Electrical Engineering, ETH Zürich, Zürich, Switzerland

ARTICLE INFO

Keywords:
Distribution grid
Parameter estimation
Smart meters
Network identification

ABSTRACT

Reliable integration and operation of renewable distributed energy resources requires accurate distribution grid models. However, obtaining precise models by field inspection is often prohibitively expensive, given their large scale and the ongoing nature of grid operations. To address this challenge, considerable efforts have been devoted to harnessing abundant consumption data for automatic model inference. The primary result of the paper is that, while the impedance of a line or a network can be estimated without synchronized phase angle measurements in a consistent way, the admittance cannot. Furthermore, a detailed statistical analysis is presented, quantifying the expected estimation errors of four prevalent admittance estimation methods. Such errors constitute fundamental model inference limitations that cannot be resolved with more data. These findings are empirically validated using synthetic data and real measurements from the town of Walenstadt, Switzerland, confirming the theory. The results contribute to our understanding of grid estimation limitations and uncertainties, offering guidance for both practitioners and researchers in the pursuit of more reliable and cost-effective solutions.

1. Introduction

The deployment of sensors and machine learning techniques on power grids has opened a new set of power system monitoring applications. Among them, line parameter and topology estimation may play a crucial role for deploying smart energy resources [1–7]. This is specially needed at the distribution level, as Distribution System Operators (DSOs) often lack accurate models of their Distribution Grids (DGs)[1]. Many recent studies have shown that physical models of a distribution grid can be estimated from synchronized voltage and current phasor measurements [8–12]. However, micro synchrophasor measurement units (μPMUs) remain expensive and therefore mostly absent in DGs.

Sensor costs motivate grid analysis that does not rely on accurate phase angle measurements, as voltage and current magnitude sensors are considerably cheaper than μPMU sensors. Smart meter sensors [13] are becoming ubiquitous for measuring power consumption. The load—coverage in European DGs is already above 70% [14]. Thus, the question whether it is possible to accurately estimate grid impedance or admittance without synchronized phase angle measurements is of practical importance. This paper investigates the feasibility of impedance and admittance estimation from voltage and current magnitude and power angle measurements only.

Given that phase angles are typically small in DGs, one might consider applying the methods used for phasor measurements with a zero angle. However, recent research demonstrates that such an approach results in an inconsistent estimate [15], even when employing Error-in-Variables (EIV) methods, e.g., the Total Least Squares (TLS). Consistency is critical when estimating DG parameters because the stability of the voltage operating point leads to a low Signal-to-Noise Ratio (SNR), which can only be mitigated by collecting a large volume of data.

Prior research has improved the accuracy of power system parameter estimation from smart meter measurements. The authors of [16] attempted to simultaneously estimating phase angles and parameters, which reduced the estimation error in some cases but did not provide consistency guarantees. A similar approach is employed in [17], where μPMUs are added at some nodes to mitigate inconsistencies, albeit not eliminating them entirely. A more recent development [18] focuses on canceling the phase variable out of the current flow equations. This

☆ This research is supported by the Swiss National Science Foundation under the NCCR Automation (grant agreement 51NF40_180545).
* Corresponding author.
E-mail addresses: jean-sebastien.brouillon@epfl.ch (J.-S. Brouillon), kmoffat@ethz.ch (K. Moffat), dorfler@ethz.ch (F. Dörfler), giancarlo.ferraritrecate@epfl.ch (G. Ferrari-Trecate).
[1] We focus on distribution network applications in this paper, however the analysis applies to transmission networks as well.

https://doi.org/10.1016/j.epsr.2024.110709
Received 1 October 2023; Received in revised form 13 March 2024; Accepted 17 June 2024
Available online 1 July 2024
0378-7796/© 2024 The Author(s). Published by Elsevier B.V. This is an open access article under the CC BY license (http://creativecommons.org/licenses/by/4.0/).

reduction yields consistent estimates of X/R ratios and certain transformations of conductance and susceptance, but not of these quantities themselves. Alternatively, some studies such as [19] have chosen to estimate impedance rather than admittance, but inverting the impedance estimates also results in accuracy issues [12].

In this paper, we aim to enhance our understanding of existing estimation methods by quantifying their inherent biases, i.e., their expected estimation errors. Our contribution can be summarized in three main aspects. We first present a detailed statistical model for common DG sensors and utilize it to express the biases associated with each estimation method in a single-line identification setup. Notably, we reveal that while each method effectively addresses certain biases from previous approaches, no admittance estimation method achieves a perfect bias cancellation, for which synchronized phasor measurements are required. Second, we show how the same reasoning can be applied to admittance matrix estimation problems when the topology is unknown. Third, to validate our findings and underscore the practical challenges of the problem, we conduct an experiment using real DG data, thereby demonstrating the applicability of the methods in the real world.

1.1. Preliminaries and notation

Complex numbers are defined as $z = a + jb$, where $a, b \in \mathbb{R}^2$ and $j^2 = -1$. The complex conjugate of $z \in \mathbb{C}$ is denoted by $z^\star$. The pseudo-inverse $A^\dagger$ of a matrix $A \in \mathbb{C}^{m\times n}$ is obtained by inverting its non-zero singular values, i.e., if $A = U\text{diag}([s, 0, \dots, 0])(V^\star)^\top$ then $A^\dagger = U\text{diag}([1/s, 0, \dots, 0])(V^\star)^\top$. If A is square and invertible, then $A^\dagger$ is equal to A^{-1} the inverse of A. The noisy measurement of a variable x is denoted by $\tilde{x}$. In a regression model $\tilde{z} = A\tilde{x}+\epsilon$, we call $\tilde{x}$ and $\tilde{z}$ the Right-Hand Side (RHS) and Left-Hand Side (LHS) variables, respectively. All variables have an implicit time-dependence, except the parameters of the network and probability distributions. This dependence is implicit. The stacked vector of $N + 1$ measurements of a variable x is denoted by $[\tilde{x}]_{t=t_0}^{t_N}$

2. System model

2.1. Distribution network

We model the power grid as a graph $\mathcal{G}(\mathcal{V}, \mathcal{E})$ with n nodes $\mathcal{V} = \{1, \dots, n\}$ and edges $\mathcal{E} \subseteq \mathcal{V} \times \mathcal{V}$. Each node $h = 1, \dots, n$ is injecting a current i_h at a voltage v_h. Consumer nodes are modeled with a negative injection. Nodal AC voltages can be expressed as phasors $v_h = |v_h|e^{j\theta_h}$, where θ_h is the phase difference with node 1. The nodal power angle ϕ_h is the phase difference between the current injection i_h and the voltage v_h (i.e., the arc cosine of the power factor). Additionally, we define all the quantities for each line $h \to k$ using a double subscript notation "hk". Thus, the voltage drop, current flow, and power angle of a line from h to k are v_{hk}, i_{hk}, and ϕ_{hk}, respectively. For convenience, we define ϕ_{hk} as the angle between i_{hk} and v_h.

Assumption 1. The voltage phase angle differences are small, i.e., $|\theta_h| \ll 1$ for all h in $\mathcal{V}$.

Comparatively small amounts of power is transmitted on DGs, which are also quite resistive. This means that Assumption 1 is quite mild. Similar to the voltages, nodal currents are also phasors $i_h = |i_h|e^{j\theta_h - j\phi_h}$, where the nodal power angle ϕ_h is not small in general.

We use a lumped-π circuit to model each electrical connection in $\mathcal{E}$ [20], where the lines are modeled as an inductor and a resistor in series, and the shunts as capacitors. This gives the line and shunt admittances $y_{hk} = g_{hk} + jb_{hk}$ and $y_{hh,s}$, respectively. If two nodes h and k are not connected, we use $y_{hk} = 0$. We assume that there are no phase-shifting transformers, and that the existing transformers have a constant tap ratio over the duration of the experiment. This means that the voltages and currents can be re-scaled to model the transformers as simple line admittances.

All parameters are collected in the admittance matrix $Y = G + jB$ with G and B in $\mathbb{R}^{n\times n}$. Y is defined by its non-diagonal elements $Y_{hk} = -y_{hk}, \forall h, k \in \mathcal{V}^2$ and its diagonal ones $Y_{kk} = \sum_{k=1}^{n} y_{hk} - y_{hh,s}, \forall h \in \mathcal{V}$. For convenience, we also define the X/R ratio $\rho_{hk} = -\frac{b_{hk}}{g_{hk}}$ of each line.[2]

2.2. Measuring devices

Smart meters provide the measurements $|\tilde{v}_h|$ and $|\tilde{i}_h|$ of the amplitudes $|v_h|$ and $|i_h|$ of the voltage and current and the measurement $\tilde{\phi}_h$ of the power angle ϕ_h [13]. However, due to the lack of GPS synchronization do not allow Smart meters to measure the voltage phase angles θ_h. Moreover, such sensors can provide the line flow measurements $\tilde{i}_{hk}$ and $\tilde{\phi}_{hk}$ if they are placed on a specific line rather than a node.

Assumption 2. The noise on the current magnitude, voltage magnitude, and power angle measurements is independent, Gaussian, and centered on zero.

Although the regulations of commercial smart meters require a given maximum admissible error, which would imply that the noise follow a truncated Gaussian [21], the resulting interval is usually large enough to approximate the noise distribution as Gaussian.

Assumption 3. The error on power angle measurement is small.

With Assumption 3, the noise on the current phasor is almost perfectly Gaussian in Cartesian coordinates. However, the real and imaginary parts of the noise on current measurements are not independent if the power angle is non-zero.

Remark 1. The active and reactive powers are not a linear combination of the measured quantities and are subject to the dependence between the real and imaginary parts of the current noise. Their uncertainty is therefore neither Gaussian-distributed nor independent, which is a common assumption in the literature.

Under Assumption 2, we can define the noise on the difference of voltage magnitudes between two nodes and its distribution as

$$\delta_{hk}^{v} := (|\tilde{v}_h| - |\tilde{v}_k|) - (|v_h| - |v_k|) \sim \mathcal{N}(0, \sigma_{hk}^{v}). \tag{1a}$$

We chose the lower-case symbol σ_{hk}^{v} for the variance to emphasize the fact that it is scalar. We also define the noise on the line current flow $|\tilde{i}_{hk}|e^{-j\tilde{\phi}_{hk}}$ measured at node h as

$$\begin{bmatrix}\delta_{hk}^{\Re}\\ \delta_{hk}^{\Im}\end{bmatrix} := \begin{bmatrix}|\tilde{i}_{hk}|\cos(\tilde{\phi}_{hk}) - |i_{hk}|\cos(\phi_{hk})\\ |\tilde{i}_{hk}|\sin(\tilde{\phi}_{hk}) - |i_{hk}|\sin(\phi_{hk})\end{bmatrix} \sim \mathcal{N}(0, \Sigma_{hk}^{i}), \tag{1b}$$

where Σ_{hk}^{i} is a 2-by-2 symmetric matrix containing the variances $\sigma_{hk}^{\Re} = \text{var}[\delta_{hk}^{\Re}]$ and $\sigma_{hk}^{\Im} = \text{var}[\delta_{hk}^{\Im}]$ of both parts of the noise on i_{hk} in the diagonal elements, and their covariance $\text{cov}[\delta_{hk}^{\Re}, \delta_{hk}^{\Im}]$ in the off-diagonal elements. Finally, we consider that the final measurements are synchronized block-averages of the instantaneous readings, and that the average over the estimation window is subtracted from each block to center the data.

3. Line parameter estimation

We first study the estimation problem for a single line before addressing network identification in Section 6.

[2] Inverting a complex number does not invert the ratio between its real and imaginary parts.

3.1. Impedance estimation

The parameters $z_{hk} = y_{hk}^{-1}$ of a line $h \to k$ relate the current flow i_{hk} to the difference of voltages $v_h - v_k$ at each end of the line according to the following relationship

$$|v_h|e^{j\theta_h} - |v_k|e^{j\theta_k} = z_{hk}|i_{hk}|e^{j(\theta_h - \phi_{hk})}, \tag{2}$$

which can be written in real numbers and linearized using $e^{-j\theta_{hk}} \approx 1 - j\theta_{hk}$ from Assumption 1 as

$$|v_h| - |v_k| = r_{hk}|i_{hk}|\cos(\phi_{hk}) + x_{hk}|i_{hk}|\sin(\phi_{hk}), \tag{3a}$$

$$|v_k|\theta_{hk} = -r_{hk}|i_{hk}|\sin(\phi_{hk}) + x_{hk}|i_{hk}|\cos(\phi_{hk}). \tag{3b}$$

Numerical evidence that (3) is a very close approximation of (2) when the currents and voltages are exact is given in [15].

The phase θ_{hk} is not measured so one must use (3a) to fit the parameters r_{hk} and x_{hk}. With noisy measurements, the regression is performed on the model

$$|\tilde{v}_h| - |\tilde{v}_k| = r_{hk}|\tilde{i}_{hk}|\cos(\tilde{\phi}_{hk}) + x_{hk}|\tilde{i}_{hk}|\sin(\tilde{\phi}_{hk}) + \epsilon_{hk}, \tag{4}$$

where $\epsilon_{hk} = \delta^v_{hk} - r_{hk}\delta^{\Re}_{hk} - x_{hk}\delta^{\Im}_{hk}$ embeds the uncertainty.

Remark 2. Under Assumption 1, (3b) ≈ 0 so one can also use (3b) as a regularizer with strength λ, by adding $-\lambda r_{hk}|\tilde{i}_{hk}|\sin(\tilde{\phi}_{hk}) + \lambda x_{hk}|\tilde{i}_{hk}|\cos(\tilde{\phi}_{hk}) \approx 0$ to the regression. This can be done by augmenting the voltage and current data matrices with $[0]_{t=t_0}^{t_N}$ and $[-\lambda|\tilde{i}_{hk}|\sin(\tilde{\phi}_{hk}), \lambda|\tilde{i}_{hk}|\cos(\tilde{\phi}_{hk})]_{t=t_0}^{t_N}$, respectively.

3.2. Admittance estimation

Similar to the impedance, the admittance relates the current flow i_{hk} to the difference of voltages $v_h - v_k$ at each end of the line, but in the inverse way. This gives following relationship

$$|i_{hk}|e^{-j\phi_{hk}} = y_{hk}\left(|v_h| - |v_k|e^{-j\theta_{hk}}\right). \tag{5}$$

As for (3), using the truncated expansion $e^{-j\theta_{hk}} \approx 1 - j\theta_{hk}$ yields

$$|i_{hk}|\cos(\phi_{hk}) = g_{hk}(|v_h| - |v_k|) - b_{hk}|v_k|\theta_{hk}, \tag{6a}$$

$$|i_{hk}|\sin(\phi_{hk}) = -g_{hk}|v_k|\theta_{hk} - b_{hk}(|v_h| - |v_k|). \tag{6b}$$

One can observe that the unobserved phase angle θ_{hk} is not simple to remove from (6) as it is done in (3). Assumption 1 hints that one could handle the missing phase measurements by replacing them with zero. However, the phase often has a key role in power transmission in practice so assuming it to be exactly zero is often too constraining. Nevertheless, for very resistive grids, inferring g_{hk} and b_{hk} in the following regression model sometimes yields good results.

$$|\tilde{i}_{hk}|\cos(\tilde{\phi}_{hk}) = g_{hk}(|\tilde{v}_h| - |\tilde{v}_k|) + \mu_{hk} - b_{hk}|v_k|\theta_{hk}, \tag{7a}$$

$$|\tilde{i}_{hk}|\sin(\tilde{\phi}_{hk}) = -b_{hk}(|\tilde{v}_h| - |\tilde{v}_k|) + \underbrace{\nu_{hk} - g_{hk}|v_k|\theta_{hk}}_{\text{considered as noise}}, \tag{7b}$$

where $\mu_{hk} = \delta^{\Re}_{hk} - g_{hk}\delta^v_{hk}$ and $\nu_{hk} = \delta^{\Im}_{hk} + b_{hk}\delta^v_{hk}$.

To conclude this section, we observe that the admittance regression model (7) actively enforces a small phase angle θ_{hk}, in contrast with the impedance regression (4).

4. Impedance estimation bias and variance

This section characterizes the bias and variance of single line impedance estimation. As described in Appendix, fitting (4) using the Ordinary Least Squares (OLS) results in biased estimates of x_{hk} and r_{hk}. This bias can be eliminated by using Total Least Squares (TLS). However, if there are correlations between the LHS and the RHS of the regression model, the TLS estimates can also be biased. Nevertheless, for the noise model (1), the TLS are a close approximation of the Maximum Likelihood Estimator (MLE), which can only be computed exactly if the phase is known.

Lemma 1. *If a regression model $\tilde{z} = A(\tilde{x} - \epsilon_x) + \epsilon_z$, where $\epsilon_x, \epsilon_x \sim \mathcal{N}(0, \Sigma)$[3] is fitted to D datasets $\tilde{x}_d, \tilde{z}_d$, the bias of the TLS is given by*

$$E[\hat{A}] - A = \left(\sum_{d=1}^{D} \text{var}[\tilde{x}_d] - \text{var}[\epsilon_{xd}]\right)^{-1} \cdot \left(\sum_{d=1}^{D} \text{cov}[\epsilon_{xd}, \epsilon_{zd}] + \text{cov}[\epsilon_{xd}, \tilde{z}_d] + \text{cov}[\tilde{x}_d, \epsilon_{zd}]\right). \tag{8}$$

Proof. The proof is derived in Appendix A.2. □

Applying Lemma 1 with $D = 1$ to the model (4) with the noise statistics (1) gives the bias

$$E[\hat{r}_{hk}] - r_{hk} = (\text{var}[|\tilde{i}_{hk}|\cos(\tilde{\phi}_{hk})] - \text{var}[\delta^{\Re}_{hk}])^{-1} \cdot (\text{cov}[\delta^{\Re}_{hk}, |\tilde{v}_h| - |\tilde{v}_k|] + \text{cov}[|\tilde{i}_{hk}|\cos(\tilde{\phi}_{hk}), \delta^v_{hk}] - \text{cov}[\delta^{\Re}_{hk}, \delta^v_{hk}]),$$

and similarly for x_{hk}. All three covariances are zero in (1) so we conclude that the TLS estimate of the impedance is unbiased. Moreover, the variance of the impedance estimate can be derived from [22] as[4]

$$\text{var}\begin{bmatrix}\hat{r}_{hk}\\ \hat{x}_{hk}\end{bmatrix} = \frac{\sigma^v_{hk} + \|[r_{hk}, x_{hk}]\|^2_{\Sigma^i_{hk}}}{N} \text{var}\begin{bmatrix}|\tilde{i}_{hk}|\cos(\tilde{\phi}_{hk})\\ |\tilde{i}_{hk}|\sin(\tilde{\phi}_{hk})\end{bmatrix}^{-1}, \tag{9}$$

where $\|[r_{hk}, x_{hk}]\|^2_{\Sigma^i_{hk}} = [r_{hk}, x_{hk}]\Sigma^i_{hk}[r_{hk}, x_{hk}]^\top$. Eq. (9) shows the consistency[5] of the TLS estimate because $\text{var}[\hat{r}_{hk}, \hat{x}_{hk}] \to 0$ as $N \to \infty$.

5. Admittance estimation bias

This section characterizes the biases of several admittance estimation methods from the literature for a single line. We focus on the limit case where the sample size is very large, because the amount of data is not a big limitation for the estimation problem. This means that although the variance can be derived from [22] (similar to (9)), we do not include it in this study because it decays to zero as $N \to \infty$ and is therefore less limiting than the biases.

The analysis demonstrates that four known methods for estimating the admittance from smart meter measurements produce biased estimates. Nevertheless, we show in Section 5.4 that, surprisingly, the biases decay with $N \to \infty$ only if one inverts the impedance estimate. Thus, if one is interested in the admittance of a line from a large data set, it may be better to estimate the impedance and then invert the estimate.

5.1. Omitted-phase bias

We start by quantifying the bias that appears when fitting the model (7) using the TLS. The magnitude difference $|\tilde{v}_h| - |\tilde{v}_k|$ is often correlated with the phase shift θ_{hk}, which means that a bias may appear if it is incorporated as noise, as explained in Section 5.3. Using Lemma 1 with $D = 1$ and the model (7a), we can express the resulting omitted-phase bias[6] with

$$E[\hat{g}_{hk}] - g_{hk} = b_{hk}(\text{var}[|\tilde{v}_h| - |\tilde{v}_k|] - \sigma^v_{hk})^{-1}\text{cov}[|\tilde{v}_h| - |\tilde{v}_k|, |v_k|\theta_{hk}],$$

and similarly for $\hat{b}_{hk}$.

[3] The RHS and LHS variables must be normalized to have the same noise variance.

[4] $\text{var}[\hat{r}_{hk}, \hat{x}_{hk}]$ depends on the exact parameters r_{hk} and x_{hk} and can, in practice, only be estimated if the SNR is sufficiently high [22].

[5] Consistent means that it converges with probability 1 to the exact parameters as $N \to \infty$. Efficient means that its variance is equal to the Camer-Rao lower bound [23].

[6] More commonly known as omitted-variable bias.

In order to avoid the omitted-phase bias, the authors of [16,17] estimate both the phase θ_{hk} and the parameters g_{hk} and b_{hk} iteratively in a joint problem. This means using the estimates $\hat{g}_{hk}$ and $\hat{b}_{hk}$ to find the estimate $\hat{e}^{\theta}_{hk}$ of $|v_k|\theta_{hk}$, which can in be plugged in (7) to update $\hat{g}_{hk}$ and $\hat{b}_{hk}$. Any method to compute $\hat{e}^{\theta}_{hk}$ will aim at satisfying (7). Rearranging the terms, vectorizing and plugging in the estimates, this means

$$\hat{e}^{\theta}_{hk}\begin{bmatrix}\hat{b}_{hk}\\ \hat{g}_{hk}\end{bmatrix}=(|\tilde{v}_h|-|\tilde{v}_k|-\delta^{v}_{hk})\begin{bmatrix}\hat{g}_{hk}\\ -\hat{b}_{hk}\end{bmatrix}-|\tilde{i}_{hk}|\begin{bmatrix}\cos(\tilde{\phi}_{hk})\\ \sin(\tilde{\phi}_{hk})\end{bmatrix}+\begin{bmatrix}\delta^{\Re}_{hk}\\ \delta^{\Im}_{hk}\end{bmatrix}. \tag{10}$$

The estimate $\hat{e}^{\theta}_{hk}$ can then be used in (7) as

$$|\tilde{i}_{hk}|\cos(\tilde{\phi}_{hk})=[g_{hk},b_{hk}][(|\tilde{v}_h|-|\tilde{v}_k|),-\hat{e}^{\theta}_{hk}]^{\top}+\mu_{hk}, \tag{11a}$$

$$|\tilde{i}_{hk}|\sin(\tilde{\phi}_{hk})=-[g_{hk},b_{hk}][\hat{e}^{\theta}_{hk},(|\tilde{v}_h|-|\tilde{v}_k|)]^{\top}+\nu_{hk}, \tag{11b}$$

While estimating θ_{hk} avoids the omitted-phase bias, it leads to a real and imaginary simultaneity bias[7], which is presented in the next section.

5.2. Real and imaginary simultaneity

A simultaneity bias appears when LHS variables in one equation appear on the RHS of another equation, hence creating correlation between the noise on the LHS and the variables in the RHS. To show that this correlation exists, we consider that the estimates are good, i.e., $[\hat{e}^{\theta}_{hk},\hat{g}_{hk},\hat{b}_{hk}]\approx[|v_k|\theta_{hk},g_{hk},b_{hk}]$. Because $[\hat{g}_{hk},\hat{b}_{hk}][g_{hk},b_{hk}]^{\dagger}\approx 1$ by construction, one obtains

$$\operatorname{cov}\big[[\delta^{\Re}_{hk},\delta^{\Im}_{hk}],\hat{e}^{\theta}_{hk}\big]\approx\operatorname{cov}\big[[\delta^{\Re}_{hk},\delta^{\Im}_{hk}],\hat{e}^{\theta}_{hk}[\hat{g}_{hk},\hat{b}_{hk}]\big][g_{hk},b_{hk}]^{\dagger}.$$

The expression (10) shows that $\hat{e}^{\theta}_{hk}$ is correlated to the noises $\delta^{\Re}_{hk}$ and $\delta^{\Im}_{hk}$. Hence,

$$\operatorname{cov}\big[[\delta^{\Re}_{hk},\delta^{\Im}_{hk}],\hat{e}^{\theta}_{hk}[\hat{g}_{hk},\hat{b}_{hk}]\big]=\operatorname{var}\begin{bmatrix}\delta^{\Re}_{hk}\\ \delta^{\Im}_{hk}\end{bmatrix},$$

which means that

$$\operatorname{cov}\big[[\delta^{\Re}_{hk},\delta^{\Im}_{hk}],\hat{e}^{\theta}_{hk}\big]\approx\Sigma^{i}_{hk}[g_{hk},b_{hk}]^{\dagger}.$$

Hence, using Lemma 1 for (11) with $D=2$ and the datasets $[|\tilde{v}_h|-|\tilde{v}_k|,-\hat{e}^{\theta}_{hk}]$, $|\tilde{i}_{hk}|\cos(\tilde{\phi}_{hk})$ and $[-\hat{e}^{\theta}_{hk},-|\tilde{v}_h|+|\tilde{v}_k|]$, $|\tilde{i}_{hk}|\sin(\tilde{\phi}_{hk})$ yields the real and imaginary simultaneity bias

$$E[\hat{b}_{hk},\hat{g}_{hk}]^{\top}-[b_{hk},g_{hk}]^{\top}\approx -\Bigg(\underbrace{\operatorname{var}\begin{bmatrix}|\tilde{v}_h|-|\tilde{v}_k|\\ -\hat{e}^{\theta}_{hk}\end{bmatrix}}_{\text{from (11a)}}+\underbrace{\operatorname{var}\begin{bmatrix}\hat{e}^{\theta}_{hk}\\ |\tilde{v}_h|-|\tilde{v}_k|\end{bmatrix}}_{\text{from (11b)}}-\begin{bmatrix}s^{e}_{hk}&0\\ 0&s^{e}_{hk}\end{bmatrix}\Bigg)^{-1}\Sigma^{i}_{hk}[g_{hk},b_{hk}]^{\dagger},$$

where $s^{e}_{hk}=\operatorname{var}[\hat{e}^{\theta}_{hk}-|\tilde{v}_k|\theta_{hk}]+\sigma^{v}_{hk}$.

The solution given in the literature [24] to the simultaneity bias is to study the reduced regression model, i.e. plugging one equation into the other, substituting the exact unknown variable rather than its estimate. This has been done in [18], where the authors reduce the equations to remove the unobserved phase θ_{hk}. We proceed similarly here, i.e., reducing $|\tilde{v}_k|\theta_{hk}$ by plugging (7b) into (7a), which gives the reduced regression model

$$\begin{aligned}|\tilde{i}_{hk}|\cos(\tilde{\phi}_{hk})=&-\rho_{hk}|\tilde{i}_{hk}|\sin(\tilde{\phi}_{hk})\\ &+g_{hk}(1+\rho^{2}_{hk})(|\tilde{v}_h|-|\tilde{v}_k|-\delta^{v}_{hk})+\rho_{hk}\delta^{\Im}_{hk}+\delta^{\Re}_{hk}.\end{aligned} \tag{12}$$

This regression gives the estimates of ρ_{hk} and $g_{hk}(1+\rho^{2}_{hk})$. The latter can then be divided by $(1+\hat{\rho}^{2}_{hk})$ to obtain an estimate of g_{hk}. A similar process can be followed for b_{hk} by plugging (7a) into (7b).

[7] The simultaneity bias problem is well known in statistics. It originates from the lack of causality between variables that occur simultaneously [24], i.e., variations in voltage and current flow.

5.3. Endogeneity of $\delta^{\Re}_{hk}$ and $\delta^{\Im}_{hk}$

We investigate the bias of TLS estimates when using the regression model (12). As explained in Section 2.2, there is a correlation between $\delta^{\Re}_{hk}$ and $\delta^{\Im}_{hk}$ when the power angle is not zero. Hence, from Lemma 1, the estimate of $\hat{\rho}_{hk}$ has the following endogeneity bias

$$E[\hat{\rho}_{hk}]-\rho_{hk}=[1,0]\cdot -\left(\operatorname{var}\begin{bmatrix}|\tilde{i}_{hk}|\sin(\tilde{\phi}_{hk})\\ |\tilde{v}_h|-|\tilde{v}_k|\end{bmatrix}-\begin{bmatrix}\sigma^{\Im}_{hk}&0\\ 0&\sigma^{v}_{hk}\end{bmatrix}\right)^{-1}\begin{bmatrix}\operatorname{cov}[\delta^{\Re}_{hk},\delta^{\Im}_{hk}]\\ 0\end{bmatrix},$$

when estimated from (12).

The removal of the endogeneity bias can be done by dividing (12) by $g_{hk}(1+\rho^{2}_{hk})$ and putting $|\tilde{v}_h|-|\tilde{v}_k|$ on the LHS. Thus, the dependence of $\delta^{\Re}_{hk}$ and $\delta^{\Im}_{hk}$ does not cross sides. Surprisingly, adjusting (12) in this way produces (4), an impedance estimate, because

$$r_{hk}=\frac{g^{-1}_{hk}}{(1+\rho^{2}_{hk})}=\left(g_{hk}+b^{2}_{hk}g^{-1}_{hk}\right)^{-1}, \tag{13a}$$

$$x_{hk}=\rho_{hk}r_{hk}=-\left(b_{hk}+g^{2}_{hk}b^{-1}_{hk}\right)^{-1}. \tag{13b}$$

5.4. Impedance inversion bias

If the goal is to estimate the admittance values, rather than the impedance values, the problem is still not fully solved as one must invert (13) to obtain the estimates of g_{hk} and b_{hk},[8]. This yields

$$g_{hk}=\left(r_{hk}+x^{2}_{hk}r^{-1}_{hk}\right)^{-1}, \tag{14a}$$

$$b_{hk}=-\left(x_{hk}+r^{2}_{hk}x^{-1}_{hk}\right)^{-1}. \tag{14b}$$

We can quantify the quality of the admittance estimate using bounds on $E[|\hat{g}_{hk}|]$ and $E[|\hat{b}_{hk}|]$, as the signs are known,[9]. To do so, we rewrite (14) as

$$\begin{aligned}|g_{hk}|&=r_{hk}(x^{2}_{hk}+r^{2}_{hk})^{-1}+x_{hk}\cdot 0,\\ |b_{hk}|&=r_{hk}\cdot 0+x_{hk}(x^{2}_{hk}+r^{2}_{hk})^{-1}.\end{aligned}$$

Plugging the functions $f_1(r,x)=(x^2+r^2)^{-1}$ and $f_2(r,x)=0$, which are convex on the positive quadrant, into a sharp[10] Jensen-like inequality [25, Theorem 2.1] gives the bounds[11]

$$E[|\hat{g}_{hk}|]\geq E[\hat{r}_{hk}]f_1\left(\frac{\operatorname{var}[\hat{r}_{hk}]}{E[\hat{r}_{hk}]}+E[\hat{r}_{hk}],\frac{\operatorname{cov}[\hat{x}_{hk},\hat{r}_{hk}]}{E[\hat{r}_{hk}]}+E[\hat{x}_{hk}]\right),$$

$$E[|\hat{b}_{hk}|]\geq E[\hat{x}_{hk}]f_1\left(\frac{\operatorname{cov}[\hat{x}_{hk},\hat{r}_{hk}]}{E[\hat{x}_{hk}]}+E[\hat{r}_{hk}],\frac{\operatorname{var}[\hat{x}_{hk}]}{E[\hat{x}_{hk}]}+E[\hat{x}_{hk}]\right),$$

where the variance of the estimates $\operatorname{var}[\hat{r}_{hk},\hat{x}_{hk}]$ is given by (9). Using the definition of $f_1(r,x)=(r^2+x^2)^{-1}$ and noting that $E[\hat{r}_{hk}]=r_{hk}$ and $E[\hat{x}_{hk}]=x_{hk}$, one gets

$$E[|\hat{g}_{hk}|]\geq\frac{r^{3}_{hk}}{(\operatorname{var}[\hat{r}_{hk}]+r^{2}_{hk})^{2}+(\operatorname{cov}[\hat{x}_{hk},\hat{r}_{hk}]+r_{hk}x_{hk})^{2}}, \tag{15a}$$

$$E[|\hat{b}_{hk}|]\geq\frac{x^{3}_{hk}}{(\operatorname{var}[\hat{x}_{hk}]+x^{2}_{hk})^{2}+(\operatorname{cov}[\hat{x}_{hk},\hat{r}_{hk}]+r_{hk}x_{hk})^{2}}. \tag{15b}$$

Because of the consistency of the TLS estimate, $\operatorname{var}[\hat{r}_{hk},\hat{x}_{hk}]\to 0$ as $N\to\infty$. This means that $\hat{g}_{hk}$ and $\hat{b}_{hk}$ can be asymptotically unbiased because the RHS of (15) tends to (14). However, with a finite number of samples, $\operatorname{var}[\hat{r}_{hk},\hat{x}_{hk}]$ can remain quite high, which may heavily bias the admittance estimate.

[8] In Section 5.2 inverting $(1+\hat{\rho}^{2}_{hk})$ also leads to a bias because ρ_{hk} is not known exactly.

[9] From the line model in Section 2.1 r_{hk} and x_{hk} are positive. One can enforce the signs of the conductance and susceptance by setting $\hat{g}_{hk}=0$ if the result was negative and $\hat{b}_{hk}=0$ if it was positive.

[10] the equality holds for at least one realization of $\hat{r}_{hk}$ and $\hat{x}_{hk}$

[11] Upper bounds were recently discovered for univariate functions [26], however there are no upper bounds yet for bivariate problems such as (14)

6. Network identification

Often, DSOs are interested in estimating the model for their full network. Ideally, the model could be estimated from smart meter injection measurements throughout the network. When a grid is radial and the topology is known, the network identification problem for the full network can be decomposed into individual line parameter estimation problems for each line using Kirchoff's Current Law. However, this is not possible for mesh networks or radial networks with unknown topologies. Thus, it is desirable to have a method for estimating the grid parameters for a full single-phase[12] network[13] from just smart meter voltage and injection measurements.

Estimating a network from just smart meter voltage and injection measurements is a much more challenging task than estimating just a single line, however, and thus requires the following additional approximation:

$$i_h \approx |i_h| e^{-j\phi_h} \qquad \text{: neglect current phase shifts.}$$

Such approximations are quite accurate if Assumption 1 is satisfied, as shown in [18]. With the aforementioned approximations, the Kirchhoff law at node h is given by $|i_h|e^{-j\phi_h} = \sum_{k=1}^{n} y_{hk}(|v_h|(1-j\theta_h)-|v_k|(1-j\theta_k))$. In matrix form and for all $h \in \mathcal{V}$, this gives

$$I^{\Re} = (G|V| - B(|V|\Theta)), \tag{16a}$$

$$I^{\Im} = -(B|V| + G(|V|\Theta)), \tag{16b}$$

where $I^{\Re} = [|i_h|\cos(\phi_h)]_{h=1}^{n}$, $I^{\Re} = [|i_h|\sin(\phi_h)]_{h=1}^{n}$, $|V| = [|v_h|]_{h=1}^{n}$, and $\Theta = [|\theta_h|]_{h=1}^{n}$. The parameter estimation problem consists in finding $G \in \mathbb{R}^{n\times n}$ and $B \in \mathbb{R}^{n\times n}$ from noisy measurements of the current magnitudes, voltage magnitudes and power angles.

6.1. Reduced regression model

Similar to [29], we use pseudo-inverses to avoid the problems caused by the singularity of Y in the absence of shunt elements. Recall that if Y is invertible, its pseudo-inverse is equal to its inverse. We first note that $BG^{\dagger}G = B$ because the matrices have the same null space[14] defined by the vector of all ones and are both rank $n-1$. Hence, multiplying (16b) by $BG^{\dagger}$ on both sides, one can rewrite (16) as

$$B(|V|\theta) = (G|V| - I^{\Re}),$$
$$B(|V|\theta) = -(BG^{\dagger}B|V| + BG^{\dagger}I^{\Im}).$$

Combining the two equations yields the reduced model

$$(G + BG^{\dagger}B)|V| = I^{\Re} - BG^{\dagger}I^{\Im}. \tag{17}$$

This model was first presented in [18], where the authors regress $|V|$ and $I^{\Im}$ onto $I^{\Re}$ to obtain $G = (G+BG^{\dagger}B)(GG^{\dagger}+(BG^{\dagger})^2)^{\dagger}$, and similarly for B. However, as explained in Section 5.3, the regression (17) suffers from a correlation between $I^{\Re}$ and $I^{\Im}$, which makes the estimation of $BG^{\dagger}$ very challenging.

[12] Three-phases networks can be identified using single-phase methods by splitting the measurement into sequences [27]. However, as the imbalances are small in practice, the zero and negative sequence data is often too ill-conditioned for identification.

[13] The "full" network that is estimated consists of the Kron-reduced network connecting just the nodes at which the injections are measured. Note, the Kron-reduction is different than the statistical reductions that are used elsewhere in this paper. The unmeasured injections are treated as noise [12,28].

[14] For this reason, the equality also holds for $GB^{\dagger}B = G$ and other combinations of these matrices, as well as their sums and products.

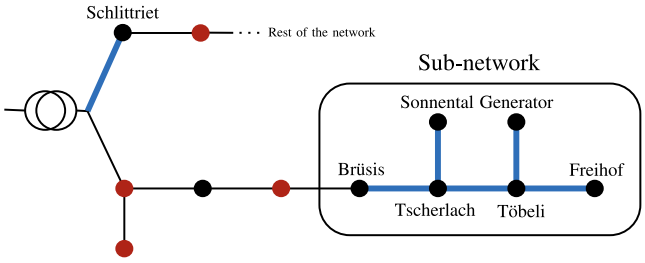

Fig. 1. Graph of the region of interest in the Walenstadt network. The lines that will be identified are in blue. The unobserved nodes are in red.

6.2. Equivalent impedance

In order to avoid the bias caused by the correlation between $I^{\Re}$ and $I^{\Im}$, we define the matrix O such that $O_{hh} = \frac{n-1}{n}$ and $O_{hk} = \frac{1}{n}$. This matrix has the same null space as G and B and has rank $n-1$. Moreover, the matrix $(G + BG^{\dagger}B)$ also has the same null space and rank, which means that $O(G + BG^{\dagger}B)^{\dagger}(G + BG^{\dagger}B) = O$. Moreover, by construction $O(G + BG^{\dagger}B)^{\dagger} = (G + BG^{\dagger}B)^{\dagger}$. We can therefore multiply both sides of (17) by $O(G + BG^{\dagger}B)^{\dagger}$ to obtain

$$O|V| = (G + BG^{\dagger}B)^{\dagger}I^{\Re} - (G + BG^{\dagger}B)^{\dagger}BG^{\dagger}I^{\Im}.$$

Finally, because $(G + BG^{\dagger}B)^{\dagger}BG^{\dagger} = (B + GB^{\dagger}G)^{\dagger}$, similar to (4) and (13), one obtains the regression

$$O|V| = RI^{\Re} + XI^{\Im}, \tag{18}$$

where

$$\begin{aligned} R &= (G + BG^{\dagger}B)^{\dagger}, \\ X &= -(B + GB^{\dagger}G)^{\dagger}, \end{aligned} \quad \Leftrightarrow \quad \begin{aligned} G &= (R + XR^{\dagger}X)^{\dagger}, \\ B &= -(X + RX^{\dagger}R)^{\dagger}. \end{aligned} \tag{19}$$

Estimating R and X using the TLS is consistent, unbiased and efficient for the same reasons as in the single line problem. Similar to Section 5.4, the pseudo-inversion of the estimates of R and X lead to an asymptotic bias. It can also be bounded using [25, Theorem 2.1]. The exact expressions are very long and are outside of the scope of this paper. Nevertheless, we show the accuracy of the estimates numerically in the next section.

7. Experiments

We validate our results on the 16 kV distribution grid of Walenstadt, Switzerland. Not all the nodes are observed/have smart meter measurements. We first use the line from the substation to Schlittriet to test the single-line identification methods. We then experiment with network identification using the Brüsis-to-Freihof six-node subnetwork. A groundtruth model of the network is not available so we assess the accuracy of the estimation methods using a combination of intuition, validation, and synthetic data, as explained below.

7.1. Single line estimation

The line of interest connecting "Schlittriet" to the substation (see Fig. 1) has a resistance of approximately 0.1 Ω.[15] Its reactance is however unknown.

7.1.1. Synthetic data single line estimation

In order to understand better the biases generated by all methods, we generate synthetic data by computing the voltages that would perfectly match the measured power for all 7 days and $y = 10 - 0.5j$ Siemens.[16] We then add an increasing amount of Gaussian noise to

[15] The linear resistivity is 114mΩ/ km and the line is 880m long. The reactance is much harder to compute as it depends on the environment of the line [30].

[16] This is an estimate of the unknown reactance, not the real value.

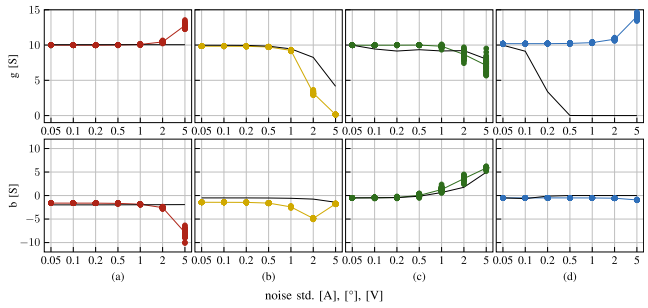

Fig. 2. Estimates of the conductance and susceptance of a single line using the four methods (a)–(d) with synthetic data. For each method, the points mark the estimates affected by one of the 50 realizations of the noise generated for each noise level. The line in color shows their average and the black line shows the predicted bias. In case (d) the black line is a lower bound on the bias.

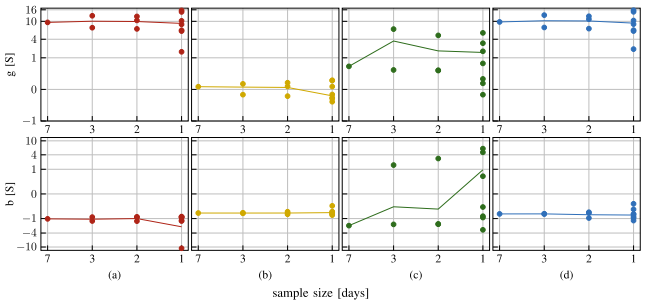

Fig. 3. Estimates of the conductance and susceptance of a single line using (a) the admittance regression (7), (b) the joint estimation using (10), (c) the reduced model (12), (d) the impedance regression (4) with real data. For each method, the points mark the estimates using each data subset and the line their average. The true conductance b and susceptance g of the line is not known, but $R \approx 0.1\ \Omega$.

observe how the estimates behave and compute the expected biases from Section 5.

Fig. 2 shows that the bias estimates accurately predict the twice too high susceptance estimate from (a), the tendency of (b) to underestimate the conductance, and the error trends of (c). However, the error of (d) is much lower than predicted because (15) is only a lower bound, and the high-noise behavior of (a) is not captured by the bias. For larger, more realistic noise levels, the bias predictions become worse because (i) infinite amounts of data would be required to compute the bias exactly and (ii) Assumption 3 may not be fully satisfied. Moreover, the approximation of $E[b]$ for (b) given in Section 5.2 is not very close. This is explained by the fact that this approximation relies on a good estimation of the phase, which is only possible with accurate parameter values. As the noise increase, the phase estimates degrade, which further increases the error in the parameter estimate.

7.1.2. Real-world data single line estimation

We use practical P, Q, and V measurements with 1% of error.[17] in all four methods described in Section 5 to obtain the results in Fig. 3. In the rest of the section, we use the sub-figure indices (a)–(d) of Fig. 3 to denote the corresponding methods. Because the true conductance and susceptance of the line is not known, we use a validation dataset in order to determine the accuracy of the methods. We split the data into 6 days for estimating the parameters, and 1 day to validate the line flow power predictions that use the parameters. Note that practical parameters are subject to variations from temperature, humidity, and loading, which further limit the estimation accuracy.

We assess the consistency of the estimates with $R = 0.1\ \Omega$, i.e., our only ground truth, by inverting the 7-days estimate using (13). We observe that (a), (c), and (d) are consistent with $R = 0.1\ \Omega$, but (b) yields $y = 0.003 - 0.46j$ S, which corresponds to an incorrect $R = 0.01\ \Omega$. Moreover, (b) and (c) estimates a much larger X/R ratio than all three other methods. The tendency of (b) to estimate g as zero is consistent with the experiment with synthetic data and can be partially explained by the bias. The larger susceptance and lower conductance estimates from method (c) are also consistent with the higher noise experiments with synthetic data. Table 1 shows that (a) provides a good estimate[18] for only P, (b) provides good estimates for only Q, and (c) does not provide a good estimate. Thus, only (d) could approximate both P and Q sufficiently well.

[17] The active and reactive powers are used to compute i_{hk} and ϕ_{hk}, which should not introduce additional error, as explained in Section 2.2 The rated voltage and power are 230 V and 250 kVA, respectively.

[18] The predictions in Table 1 are a useful validation albeit quite inaccurate. In practice, more powerful tools for line flow estimation are available [31]. In this work, the P and Q predictions are mostly used as a cross-validation tool to tune the regularization from Remark 2.

Table 1
Power transmission in the estimated line for the last day of the data. The predictions (a), (b), (c), and (d) are given by $P + jQ \approx (|\tilde{v}_h| - |\tilde{v}_k|)^2 \hat{y}_{hk} e^{j\phi_{hk}}$ using $\hat{y}_{hk}$ from each method.

	Method	P [kW]	Q [kVA]
	Measured	107.49	5.19
(a)	Admittance (7)	138.69	13.34
(b)	Joint (10)	0.044	6.98
(c)	Reduced (12)	15.62	47.08
(d)	Impedance (4)	140.34	6.63

7.2. Network identification

We now apply the results of Section 6 to the sub-network indicated in Fig. 1 in order to estimate its admittance matrix.

7.2.1. Synthetic data network identification

Similar to Section 7.1, we first compare the methods using synthetic data. To do so, because the true matrix is unknown, we use the arbitrary yet realistic admittance matrix Y_s, of which the element-wise magnitude is shown in Fig. 4(e). In order to ensure a perfect linearization such that Assumption 1 is not needed, we generate synthetic voltage profiles as $V = |(I^{\Re} + jI^{\Im})Y_s^{\dagger}|$. We ensure that Assumptions 2 and 3 are satisfied by adding 1% of Gaussian noise to the current and voltage profiles. Estimating Y_s with this data yields the following results:

(a) from [15] diverges with both OLS and TLS, yielding a quasi-infinite admittance estimate.
(b) from [16] converges to zero.
(c) from [18] diverges with the TLS but results in the matrix shown in Fig. 4(c).
(d) using (18) yields the matrix shown in Fig. 4(d) with the TLS and a similar one with the OLS.

One key observation from Fig. 4 is that the "Generator" node is wrongly connected to many nodes. We can explain this by the relatively large amounts of reactive power injected in and out of the network by this node, leading to a power angle that varies between −60 and +60 degrees. As the grid is mostly resistive, this means that most of the signal lies in the unobserved phase of the voltages. The reactive injections also explains the poor performance of method (c), as the power angle is the source of the endogeneity described in Section 5.3.

7.2.2. Real-world data network identification

We use V, P and Q measurements from real smart meters installed on the sub-network Fig. 1. The singular values of $[V, I^{\Re}, I^{\Im}]$ reveal a SNR of approximately 1, which makes the estimation challenging.

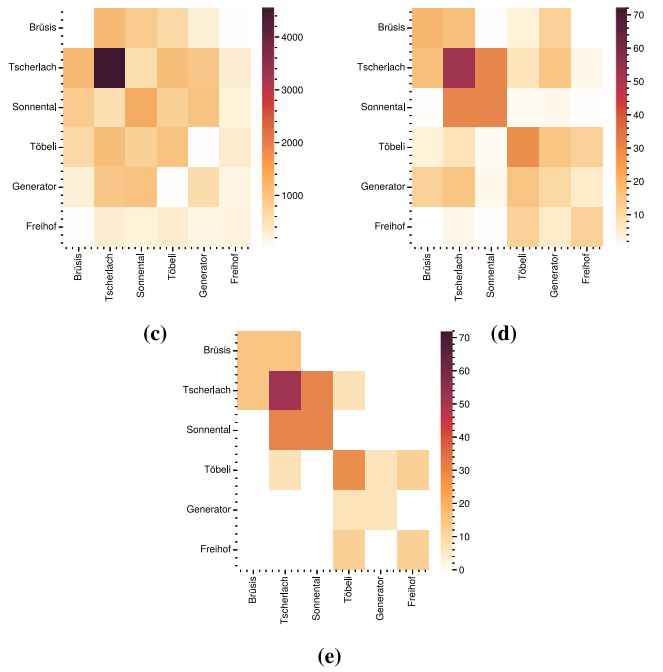

Fig. 4. Heatmaps of the magnitudes of the admittance matrix estimates given by the methods (c) and (d) with synthetic data, as well as the synthetic ground truth (e).

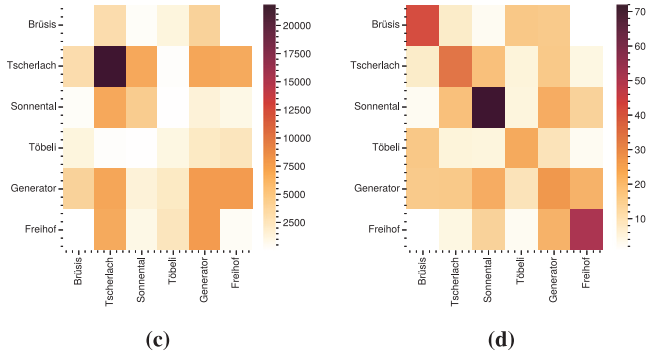

Fig. 5. Heatmaps of the magnitudes of the admittance matrix estimates given by the methods (c) and (d).

In order to avoid numerical stability issues,[19] we test the TLS-based methods with OLS as well. The estimation with all 7 days of data yields results similar to Section 7.2.1 for all methods. The estimates of methods (c) and (d) are reported in Fig. 5.

We highlight that, while the admittance matrix given in Fig. 4(e) is not the practical one, it should have the same order of magnitude, which only the method (d) achieves. Moreover, while the topology is not recognizable from Fig. 5(d), the estimate may be useful for control and state estimation purposes. If it is not, the data must be improved by installing more accurate smart meter sensors, μPMUs, or lineflow measurements.

7.3. Discussion

Estimating electrical grid parameters without μPMUs is challenging. This paper quantifies this challenge by showing that while impedance estimation can be unbiased, admittance estimation contains a non-zero expected error when using four common methods in the literature. This means that if enough data is used, adding more measurements does not improve accuracy and other types of knowledge may be required. Some μPMUs may be present at a few nodes. Including the phase measurements using (3b) may be necessary. In practice, one may know the topology and the length or type of some of the lines. which can be included as a Bayesian prior [27].

[19] In high SNR scenarios, the TLS may fail to estimate the EIV correctly and remove parts of the signal instead. While the OLS is biased, it is more robust than the TLS.

8. Conclusion

Estimating electrical grid parameters without phase measuring devices is challenging. This paper quantifies this challenge by describing the non-zero expected admittance estimation error for four admittance estimation methods in the literature, as well as the variance of impedance estimation. Impedance estimation can be conducted without bias using TLS. The results in this paper warrant further impedance and admittance estimation experiments with real smart meter data, and experiments that combine smart meter data with prior knowledge or data from other types of sensors such as uPMUs and lineflow measurements.

CRediT authorship contribution statement

Jean-Sébastien Brouillon: Data curation, Formal analysis, Investigation, Methodology, Software, Writing – original draft, Writing – review & editing. **Keith Moffat:** Conceptualization, Formal analysis, Investigation, Validation, Writing – original draft, Writing – review & editing. **Florian Dörfler:** Funding acquisition, Resources, Supervision, Validation. **Giancarlo Ferrari-Trecate:** Funding acquisition, Resources, Supervision, Validation.

Declaration of competing interest

The authors declare the following financial interests/personal relationships which may be considered as potential competing interests: Jean-Sebastien Brouillon reports financial support was provided by Swiss National Science Foundation. Keith Moffat reports was provided by Swiss National Science Foundation. Florian Dorfler reports was provided by Swiss National Science Foundation. Giancarlo Ferrari Trecate reports was provided by Swiss National Science Foundation.

Data availability

The authors do not have permission to share data.

Acknowledgments

We thank the Swiss National Science Foundation for supporting this research under the NCCR Automation project (grant number 51NF40 180545). We would also like to thank Benjamin Sawicki and WEW (the DSO of Walenstadt) for providing the data required by our experiments. Additionally, we thank Lisa Laurent and Paul Dené for the eye-opening results that they found during their Master projects.

Appendix. Dilution bias and total least squares

We explore different methods to fit regression models such as (4) or (7a). In order to present the theory in various cases, we consider a general regression model $\tilde{z} = Ax + \epsilon$. For example, in (4) z represents the voltage drop and x represents the current. The matrix A contains the parameters and the noise term ϵ is such that $E[\epsilon] = 0$.

A.1. Dilution bias

The OLS are a very common method for parameter estimation, which estimates A as

$$\hat{A} = \mathrm{var}[x]^{-1}\mathrm{cov}[x, \tilde{z}]. \tag{20}$$

This estimate is exact if (i) the variance and covariance estimates are exact and (ii) $\mathrm{cov}[x, \epsilon] = 0$, which means $\mathrm{cov}[x, \tilde{z}] = A\mathrm{var}[x]$. The condition (i) is usually almost satisfied with very large amounts of data, as the uncertainty on variance scales with the inverse of the number of samples.

The condition (ii) is not satisfied in (4) and (7a), as the noises on $|\tilde{v}_h| - |\tilde{v}_k|$, $|\tilde{i}_{hk}|\cos(\tilde{\phi}_{hk})$, and $|\tilde{i}_{hk}|\sin(\tilde{\phi}_{hk})$ are collected in ϵ_{hk}, thus creating correlations. Independent uncertainty in the measurement $\tilde{x}$ of x, then $\mathrm{var}[\tilde{x}] = \mathrm{var}[x] + \mathrm{var}[\tilde{x} - x]$, so $\mathrm{var}[\tilde{x}]^{-1} \prec \mathrm{var}[x]^{-1}$, which leads to a dilution bias in the OLS [32].

A.2. Total least squares

The TLS estimate the parameters A and the exact variance $\mathrm{var}[x]$ simultaneously, assuming that $\epsilon = \epsilon_z + \epsilon_x \sim \mathcal{N}(0, \Sigma_z) + \mathcal{N}(0, A\Sigma_z A^\top)$, i.e., that the right and left hand side variables are i.i.d., Gaussian and centered on zero. The variance $\mathrm{var}[x]$ is computed as $\mathrm{var}[\tilde{x}] - \mathrm{var}[\epsilon_x]$, where $\mathrm{var}[\epsilon_x]$ is obtained using a low-rank approximation of $[x+\epsilon_x, z+\epsilon_z]$ [32][20]. In this case, (20) becomes

$$\hat{A} = (\mathrm{var}[\tilde{x}] - \mathrm{var}[\epsilon_x])^{-1}\mathrm{cov}[\tilde{x}, \tilde{z}]. \tag{21}$$

This estimate is unbiased if and only if $\mathrm{cov}[\tilde{x}, \tilde{z}] = \mathrm{cov}[x, z] + \mathrm{cov}[\epsilon_x, \tilde{z}] + \mathrm{cov}[\tilde{x}, \epsilon_z] - \mathrm{cov}[\epsilon_x, \epsilon_z] = \mathrm{cov}[x, z]$. Otherwise the bias is given by $(\mathrm{var}[\tilde{x}] - \mathrm{var}[\epsilon_x])^{-1}(\mathrm{cov}[\tilde{x}, \tilde{z}] - \mathrm{cov}[x, z])$, which is equal to (8) when $D = 1$.

A.3. Multiple datasets

If D datasets $\tilde{x}_d, \tilde{z}_d$ of equal size such that $z_d = Ax_d$ for $d = 1, \dots, D$ are combined, (20) becomes $\hat{A} = \left(\sum_{d=1}^{D} \mathrm{var}[x_d]\right)^{-1} \sum_{d=1}^{D} \mathrm{cov}[x_d, \tilde{z}_d]$. Moreover, similar to (21), the TLS estimate uses $\mathrm{var}[x_d] = \mathrm{var}[\tilde{x}_d] - \mathrm{var}[\tilde{x}_d - x_d]$ when the noise is independent. Hence the bias is $\left(\sum_{d=1}^{D} \mathrm{var}[x_d] - \mathrm{var}[\tilde{x}_d - x_d]\right)^{-1} \sum_{d=1}^{D} (\mathrm{cov}[\tilde{x}_d, \tilde{z}_d] - \mathrm{cov}[x_d, z_d])$, which is equal to (8).

References

[1] Quadrennial Energy Review Report, Tech. Rep., IEEE Power and Energy Society, 2015.

[2] Developing Innovative Technologies to Enhance Reliability, Ensure Resilience, and Increase Flexibility, Tech. Rep., US Department of Energy, 2017.

[3] K. Morrissey, Fundamental Research Challenges for Distribution State Estimation to Enable High-Performing Grids, Tech. Rep., Smarter Grid Solutions, 2018.

[4] L. Schenato, G. Barchi, D. Macii, R. Arghandeh, K. Poolla, A. Von Meier, Bayesian linear state estimation using smart meters and pmus measurements in distribution grids, in: 2014 IEEE International Conference on Smart Grid Communications, SmartGridComm, 2014, pp. 572–577.

[5] A. Iovine, T. Rigaut, G. Damm, E. De Santis, M.D. Di Benedetto, Power management for a DC MicroGrid integrating renewables and storages, Control Eng. Pract. 85 (2019) 59–79.

[6] Flexible Export Limits-Final response and proposed actions-July 2023, Tech. Rep., Australian Energy Regulator, 2023.

[7] M.Z. Liu, L.N. Ochoa, Project EDGE–Knowledge Sharing Report: Electrical Model Validation and Operating Envelope Calculation, Tech. Rep., 2023.

[8] O. Ardakanian, V.W.S. Wong, R. Dobbe, S.H. Low, A. von Meier, C.J. Tomlin, Y. Yuan, On identification of distribution grids, IEEE Trans. Control Netw. Syst. 6 (3) (2019) 950–960.

[9] E. Fabbiani, P. Nahata, G.D. Nicolao, G. Ferrari-Trecate, Identification of AC networks via online learning, IEEE Trans. Control Syst. Technol. (2021).

[10] R. Arghandeh, M. Gahr, A. von Meier, G. Cavraro, M. Ruh, G. Andersson, Topology detection in microgrids with micro-synchrophasors, in: 2015 IEEE Power & Energy Society General Meeting, IEEE, 2015, pp. 1–5.

[11] A. Wehenkel, A. Mukhopadhyay, J.-Y. Le Boudec, M. Paolone, Parameter estimation of three-phase untransposed short transmission lines from synchrophasor measurements, IEEE Trans. Instrum. Meas. 69 (9) (2020) 6143–6154.

[12] K. Moffat, M. Bariya, A. Von Meier, Unsupervised impedance and topology estimation of distribution networks—Limitations and tools, IEEE Trans. Smart Grid 11 (1) (2020) 846–856.

[13] K. Weranga, S. Kumarawadu, D. Chandima, Smart Metering Design and Applications, Springer, 2014.

[14] S. Vitiello, N. Andreadou, M. Ardelean, G. Fulli, Smart metering roll-out in europe: Where do we stand? cost benefit analyses in the clean energy package and research trends in the green deal, Energies 15 (7) (2022) 2340.

[15] L. Laurent, J.-S. Brouillon, G. Ferrari-Trecate, Maximum likelihood estimation of distribution grid topology and parameters from smart meter data, in: 2023 IEEE PES Grid Edge Technologies Conference & Exposition, Grid Edge, IEEE, 2023, pp. 1–5.

[16] J. Zhang, Y. Wang, Y. Weng, N. Zhang, Topology identification and line parameter estimation for non-PMU distribution network: A numerical method, IEEE Trans. Smart Grid 11 (5) (2020) 4440–4453.

[17] V.L. Srinivas, J. Wu, Topology and parameter identification of distribution network using smart meter and μPMU measurements, IEEE Trans. Instrum. Meas. 71 (2022) 1–14.

[18] J. Zhang, P. Wang, N. Zhang, Distribution network admittance matrix estimation with linear regression, IEEE Trans. Power Syst. 36 (5) (2021) 4896–4899.

[19] M. Vanin, F. Geth, R. D'hulst, D. Van Hertem, Combined unbalanced distribution system state and line impedance matrix estimation, Int. J. Electr. Power Energy Syst. 151 (2023) 109155.

[20] P. Kundur, Power System Stability and Control, CRC Press New York, NY, USA, 2007.

[21] Q. Cetina, R.A.J. Roscoe, P.S. Wright, Challenges for smart electricity meters due to dynamic power quality conditions of the grid: A review, in: 2017 IEEE International Workshop on Applied Measurements for Power Systems, AMPS, IEEE, 2017, pp. 1–6.

[22] J. Crassidis, Y. Cheng, Error-covariance analysis of the total least squares problem, J. Guid. Control Dyn. 37 (2014).

[23] G. Casella, R. Berger, Statistical Inference, Duxbury Press, 2002.

[24] J.M. Wooldridge, Introductory Econometrics: A Modern Approach, Cengage learning, 2015.

[25] R.A. Agnew, J.E. Pecaric, Generalized multivariate jensen-type inequality, JIPAM. J. Inequal. Pure Appl. Math. [electronic only] 7 (4) (2006) Paper–No.

[26] J. Liao, A. Berg, Sharpening Jensen's inequality, Amer. Statist. (2018).

[27] J.-S. Brouillon, E. Fabbiani, P. Nahata, K. Moffat, F. Dörfler, G. Ferrari-Trecate, Bayesian error-in-variables models for the identification of distribution grids, IEEE Trans. Smart Grid 14 (2) (2022) 1289–1299.

[28] F. Dörfler, J.W. Simpson-Porco, F. Bullo, Electrical networks and algebraic graph theory: Models, properties, and applications, Proc. IEEE 106 (5) (2018) 977–1005.

[29] O. Stanojev, L. Werner, S. Low, G. Hug, Tractable identification of electric distribution networks, 2023, arXiv preprint arXiv:2304.01615.

[30] J.R. Carson, Electromagnetic theory and the foundations of electric circuit theory 1, Bell Syst. Tech. J. 6 (1) (1927) 1–17.

[31] K.D. Smith, F. Seccamonte, A. Swami, F. Bullo, Physics-informed implicit representations of equilibrium network flows, Adv. Neural Inf. Process. Syst. 35 (2022) 7211–7221.

[32] I. Markovsky, S. Van Huffel, Overview of total least-squares methods, Signal Process. 87 (10) (2007) 2283–2302.

[33] S. Rhode, F. Bleimund, F. Gauterin, Recursive generalized total least squares with noise covariance estimation, IFAC Proc. Vol. 47 (3) (2014) 4637–4643.

[20] The TLS can also be computed online using its recursive formulation [33]